

Supporting Information:

Effect of conformational disorder on exciton states of an azobenzene aggregate

Evgenii Titov*

*Theoretical Chemistry, Institute of Chemistry, University of Potsdam,
Karl-Liebknecht-Straße 24-25, 14476 Potsdam, Germany*

E-mail: titov@uni-potsdam.de

Contents

SI1	Details on models, methods, and calculations	S2
SI2	B3LYP+D3(BJ) dynamics	S5
SI2.1	Brightest $\pi\pi^*$ transition	S9
SI2.2	$S_0 \rightarrow S_5$ transition	S12
SI2.3	Brightest $n\pi^*$ transition	S16
SI3	ωB97X-D dynamics	S19
SI3.1	Brightest $\pi\pi^*$ transition	S23
SI3.2	$S_0 \rightarrow S_5$ transition	S26
SI3.3	Brightest $n\pi^*$ transition	S29
SI4	Exciton–vibration coupling	S32

SI1 Details on models, methods, and calculations

The tetramer model was constructed from the B3LYP/def2-TZVP optimized monomer geometry by translating this geometry by 3.5 Å in the direction perpendicular to the molecular plane of *trans* azobenzene. This tetramer geometry was used as an input geometry for BOMD simulations. The BOMD simulations were performed using B3LYP+D3(BJ) and ω B97X-D functionals with the def2-SV(P) basis set. The velocity Verlet algorithm was used to integrate Newton’s equations of motion. The time step was set to 0.5 fs and the trajectories were run up to 10 ps. The constant-temperature dynamics were simulated using a simple velocity rescaling approach, i.e. multiplying velocities by $\sqrt{\frac{T_{ref}}{T_{curr}}}$ at each time step. Here, T_{ref} is the reference (desired) temperature and T_{curr} is the current (instantaneous) temperature. The initial velocities were randomly sampled from a uniform distribution and scaled to yield the reference temperature (300 K in our case). The constant-energy trajectories were launched with zero initial velocities. Snapshots selected between 100 fs and 10 ps (with 100 fs period) were subjected to TD-DFT calculations. The excited states were calculated using TD- ω B97X-D and TD- ω B97 with def2-SV(P) basis set. The 20 lowest excited states were requested in the case of the tetramer, and 5 states in the case of the monomer. Transition density matrices were calculated using Multiwfn 3.8.

The calculated stick spectra are broadened with Gaussians as

$$I(E) = \frac{1}{N_s} \sum_i f_{i,\alpha} \exp\left(-\frac{1}{2\sigma^2} (E - E_{i,\alpha})^2\right) . \quad (\text{S1})$$

Here, I is intensity, E is excitation energy, N_s is the number of selected snapshots, $E_{i,\alpha}$ and $f_{i,\alpha}$ are the TD-DFT excitation energy and oscillator strength, respectively, for the $S_0 \rightarrow S_i$ transition, for snapshot α , and σ is a broadening parameter ($\sigma = 0.05$ eV in this work). For each selected snapshot we also calculate the spectra of four monomers forming the aggregate (to calculate the broadened spectrum of the monomer, $4N_s$ instead N_s is used in the denominator of eq. (S1)).

Since the def2-SV(P) basis set was used in dynamics and TD-DFT calculations, we have also considered the tetramer geometry constructed from the B3LYP/def2-SV(P) optimized monomer geometry. The effect of the monomer geometry on the spectra is shown in Fig. S1. While broadened spectra merely show a shift, the stick spectra of the tetramer are quite different. There is a single very intense transition ($S_0 \rightarrow S_{13}$) for the def2-SV(P) geometry, and there are two less intense closely lying transitions ($S_0 \rightarrow S_{12}$ and $S_0 \rightarrow S_{13}$) for the def2-TZVP geometry. The FTDM matrices of these transitions are shown in Fig. S2. It is seen that there is a strong admixture of CT excitations for the def2-TZVP geometry.

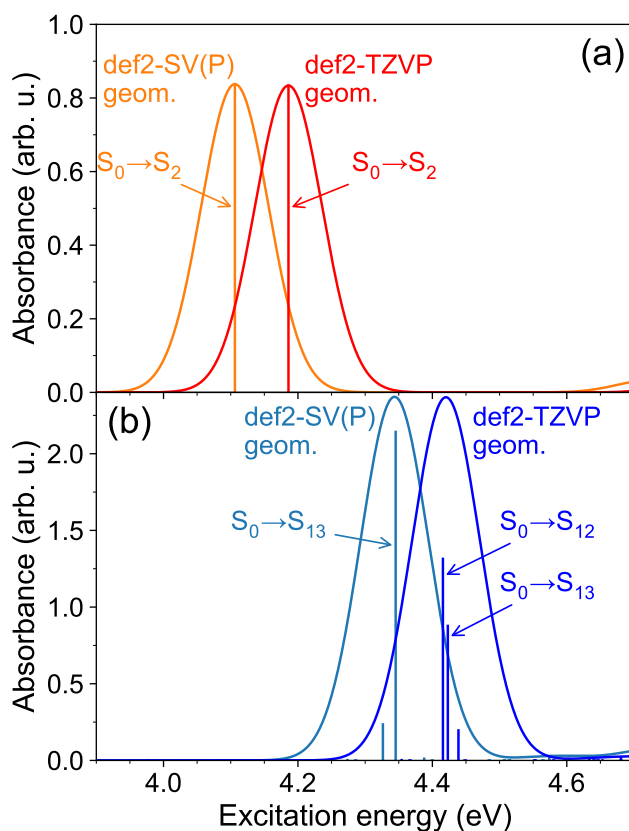


Figure S1: The $\pi\pi^*$ absorption bands of the monomer (a) and the tetramer (b) calculated with TD- ω B97X-D/def2-SV(P) at B3LYP/def2-SV(P) and B3LYP/def2-TZVP geometries.

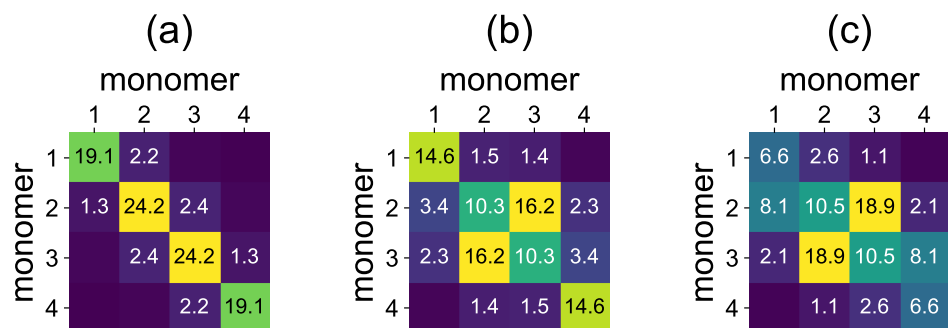


Figure S2: (a) The \mathbf{F} matrix for the $S_0 \rightarrow S_{13}$ transition of the tetramer constructed from the B3LYP/def2-SV(P) optimized monomer geometry. (b,c) The \mathbf{F} matrices for the $S_0 \rightarrow S_{12}$ (b) and $S_0 \rightarrow S_{13}$ (c) transitions of the tetramer constructed from the B3LYP/def2-TZVP optimized monomer geometry. Excited states are calculated with TD- ω B97X-D/def2-SV(P).

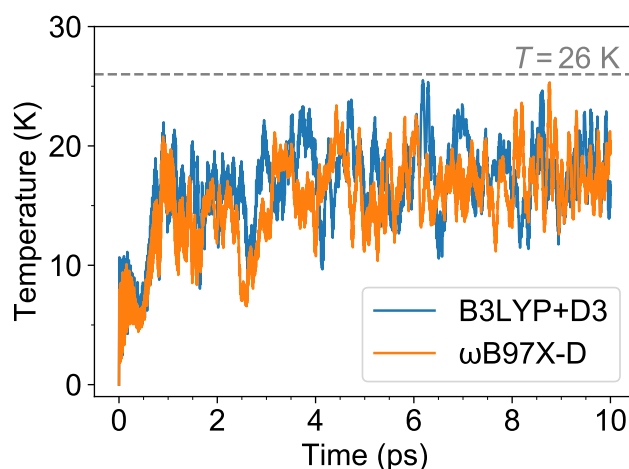


Figure S3: Instantaneous temperature as a function of time for dynamics starting from the model geometry with zero velocities. The results for B3LYP+D3 and ω B97X-D dynamics are shown.

SI2 B3LYP+D3(BJ) dynamics

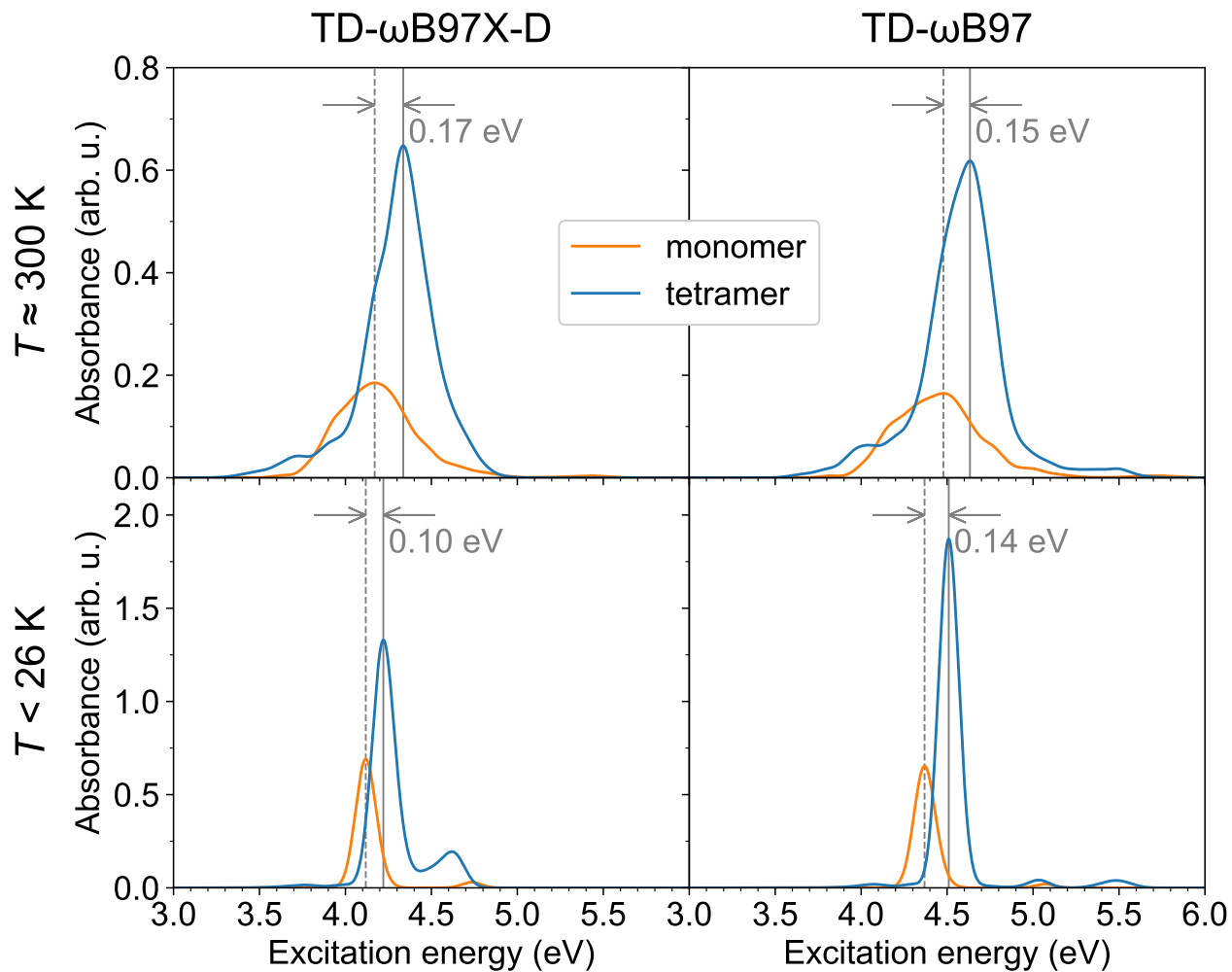


Figure S4: The $\pi\pi^*$ absorption band of the monomer and the tetramer at $T \approx 300$ K (upper row) and $T < 26$ K (lower row) calculated with TD- ω B97X-D/def2-SV(P) (left column) and TD- ω B97/def2-SV(P) (right column). The monomer-to-tetramer spectral shifts are also shown.

Figure S5: The absorption band of the monomer and the tetramer at $T = 300$ K (upper row) and $T < 26$ K (lower row) calculated with TD-B97X-D/def2-SV(P) (left column) and TD-B97/def2-SV(P) (right column). The monomer-to-tetramer spectral shifts are also shown.

Figure S6: Distributions of the brightest state label.

Figure S7: Distributions of the oscillator strength of the brightest transition.

S12.1 Brightest transition

Figure S8: TD-B97/def2-SV(P) calculations. Upper row: calculations for single (B3LYP/def2-SV(P)) geometry, for the brightest transition ($S_0 \rightarrow S_{10}$). (a) The F matrix. (b) Diagonal F_{xx} elements as well as the sum of diagonal (LE) and o-diagonal (CT) elements. Lower row: calculations for the ensemble of 100 snapshots (at 300 K), for the brightest transitions. (c) The F matrix averaged over all snapshots. (d) Diagonal F_{xx} elements of the averaged F matrix, as well as the sum of diagonal (LE) and o-diagonal (CT) elements. (e) Averaged highest to lowest diagonal values and their sum (LE). (f) Relative frequency with which monomers have the highest or lowest F_{xx} value.

Figure S9: TD! B97X-D/def2-SV(P) calculations, $T < 26$ K. (a) The F matrix averaged over all snapshots. (b) Diagonal F_{XX} elements of the averaged F matrix, as well as the sum of diagonal (LE) and o-diagonal (CT) elements. (c) Averaged highest to lowest diagonal values and their sum (LE). (d) Relative frequency with which monomers have the highest or lowest F_{XX} value.

Figure S10: TD! B97/def2-SV(P) calculations, $T < 26$ K. (a) The F matrix averaged over all snapshots. (b) Diagonal F_{XX} elements of the averaged F matrix, as well as the sum of diagonal (LE) and o-diagonal (CT) elements. (c) Averaged highest to lowest diagonal values and their sum (LE). (d) Relative frequency with which monomers have the highest or lowest F_{XX} value.

Figure S11: Inverse participation ratios for 100 snapshots.

S12.2 $S_0 \rightarrow S_5$ transition

Figure S12: TD-B3LYP/def2-SV(P) calculations. Upper row: calculations for single (B3LYP/def2-SV(P)) geometry, for the $S_0 \rightarrow S_5$ transition. (a) The F matrix. (b) Diagonal F_{XX} elements as well as the sum of diagonal (LE) and off-diagonal (CT) elements. Lower row: calculations for the ensemble of 100 snapshots (at 300 K), for the brightest transitions. (c) The F matrix averaged over all snapshots. (d) Diagonal F_{XX} elements of the averaged F matrix, as well as the sum of diagonal (LE) and off-diagonal (CT) elements. (e) Averaged highest to lowest diagonal values and their sum (LE). (f) Relative frequency with which monomers have the highest or lowest F_{XX} value.

Figure S13: TD-B97/def2-SV(P) calculations. Upper row: calculations for single (B3LYP/def2-SV(P)) geometry, for the $S_0 \rightarrow S_5$ transition. (a) The F matrix. (b) Diagonal F_{xx} elements as well as the sum of diagonal (LE) and off-diagonal (CT) elements. Lower row: calculations for the ensemble of 100 snapshots (at 300 K), for the brightest transitions. (c) The F matrix averaged over all snapshots. (d) Diagonal F_{xx} elements of the averaged F matrix, as well as the sum of diagonal (LE) and off-diagonal (CT) elements. (e) Averaged highest to lowest diagonal values and their sum (LE). (f) Relative frequency with which monomers have the highest or lowest F_{xx} value.

Figure S14: TD! B97X-D/def2-SV(P) calculations, $T < 26$ K. (a) The F matrix averaged over all snapshots. (b) Diagonal F_{XX} elements of the averaged F matrix, as well as the sum of diagonal (LE) and o-diagonal (CT) elements. (c) Averaged highest to lowest diagonal values and their sum (LE). (d) Relative frequency with which monomers have the highest or lowest F_{XX} value.

Figure S15: TD! B97/def2-SV(P) calculations, $T < 26$ K. (a) The F matrix averaged over all snapshots. (b) Diagonal F_{XX} elements of the averaged F matrix, as well as the sum of diagonal (LE) and o-diagonal (CT) elements. (c) Averaged highest to lowest diagonal values and their sum (LE). (d) Relative frequency with which monomers have the highest or lowest F_{XX} value.

Figure S16: Inverse participation ratios for 100 snapshots.

S12.3 Brightest n transition

Figure S17: TD! B97/def2-SV(P) calculations, $T = 300$ K. (a) The F matrix averaged over all snapshots. (b) Diagonal F_{XX} elements of the averaged F matrix, as well as the sum of diagonal (LE) and o-diagonal (CT) elements. (c) Averaged highest to lowest diagonal values and their sum (LE). (d) Relative frequency with which monomers have the highest or lowest F_{XX} value.

Figure S18: TD! B97X-D/def2-SV(P) calculations, $T < 26$ K. (a) The F matrix averaged over all snapshots. (b) Diagonal F_{XX} elements of the averaged F matrix, as well as the sum of diagonal (LE) and o-diagonal (CT) elements. (c) Averaged highest to lowest diagonal values and their sum (LE). (d) Relative frequency with which monomers have the highest or lowest F_{XX} value.

Figure S19: TD! B97/def2-SV(P) calculations, $T < 26$ K. (a) The F matrix averaged over all snapshots. (b) Diagonal F_{xx} elements of the averaged F matrix, as well as the sum of diagonal (LE) and o-diagonal (CT) elements. (c) Averaged highest to lowest diagonal values and their sum (LE). (d) Relative frequency with which monomers have the highest or lowest F_{xx} value.

Figure S20: Inverse participation ratios for 100 snapshots.

SI3 ! B97X-D dynamics

Figure S21: The absorption band of the monomer and the tetramer at $T = 300$ K (upper row) and $T < 26$ K (lower row) calculated with TD-! B97X-D/def2-SV(P) (left column) and TD-! B97/def2-SV(P) (right column). The monomer-to-tetramer spectral shifts are also shown.

Figure S22: The absorption band of the monomer and the tetramer at $T = 300$ K (upper row) and $T < 26$ K (lower row) calculated with TD-B97X-D/def2-SV(P) (left column) and TD-B97/def2-SV(P) (right column). The monomer-to-tetramer spectral shifts are also shown.

Figure S23: Distributions of the brightest state label.

Figure S24: Distributions of the oscillator strength of the brightest transition.

S13.1 Brightest transition

Figure S25: TD! B97X-D/def2-SV(P) calculations, $T = 300$ K. (a) The F matrix averaged over all snapshots. (b) Diagonal F_{XX} elements of the averaged F matrix, as well as the sum of diagonal (LE) and o-diagonal (CT) elements. (c) Averaged highest to lowest diagonal values and their sum (LE). (d) Relative frequency with which monomers have the highest or lowest F_{XX} value.

Figure S26: TD! B97/def2-SV(P) calculations, $T = 300$ K. (a) The F matrix averaged over all snapshots. (b) Diagonal F_{XX} elements of the averaged F matrix, as well as the sum of diagonal (LE) and o-diagonal (CT) elements. (c) Averaged highest to lowest diagonal values and their sum (LE). (d) Relative frequency with which monomers have the highest or lowest F_{XX} value.

Figure S27: TD! B97X-D/def2-SV(P) calculations, $T < 26$ K. (a) The F matrix averaged over all snapshots. (b) Diagonal F_{XX} elements of the averaged F matrix, as well as the sum of diagonal (LE) and o-diagonal (CT) elements. (c) Averaged highest to lowest diagonal values and their sum (LE). (d) Relative frequency with which monomers have the highest or lowest F_{XX} value.

Figure S28: TD! B97/def2-SV(P) calculations, $T < 26$ K. (a) The F matrix averaged over all snapshots. (b) Diagonal F_{XX} elements of the averaged F matrix, as well as the sum of diagonal (LE) and o-diagonal (CT) elements. (c) Averaged highest to lowest diagonal values and their sum (LE). (d) Relative frequency with which monomers have the highest or lowest F_{XX} value.

Figure S29: Inverse participation ratios for 100 snapshots.

S13.2 $S_0 \rightarrow S_5$ transition

Figure S30: TD-B97X-D/def2-SV(P) calculations, $T = 300$ K. (a) The F matrix averaged over all snapshots. (b) Diagonal F_{XX} elements of the averaged F matrix, as well as the sum of diagonal (LE) and off-diagonal (CT) elements. (c) Averaged highest to lowest diagonal values and their sum (LE). (d) Relative frequency with which monomers have the highest or lowest F_{XX} value.

Figure S31: TD-B97/def2-SV(P) calculations, $T = 300$ K. (a) The F matrix averaged over all snapshots. (b) Diagonal F_{XX} elements of the averaged F matrix, as well as the sum of diagonal (LE) and off-diagonal (CT) elements. (c) Averaged highest to lowest diagonal values and their sum (LE). (d) Relative frequency with which monomers have the highest or lowest F_{XX} value.

Figure S32: TD! B97X-D/def2-SV(P) calculations, $T < 26$ K. (a) The F matrix averaged over all snapshots. (b) Diagonal F_{XX} elements of the averaged F matrix, as well as the sum of diagonal (LE) and o-diagonal (CT) elements. (c) Averaged highest to lowest diagonal values and their sum (LE). (d) Relative frequency with which monomers have the highest or lowest F_{XX} value.

Figure S33: TD! B97/def2-SV(P) calculations, $T < 26$ K. (a) The F matrix averaged over all snapshots. (b) Diagonal F_{XX} elements of the averaged F matrix, as well as the sum of diagonal (LE) and o-diagonal (CT) elements. (c) Averaged highest to lowest diagonal values and their sum (LE). (d) Relative frequency with which monomers have the highest or lowest F_{XX} value.

Figure S34: Inverse participation ratios for 100 snapshots.

SI3.3 Brightest $n\pi^*$ transition

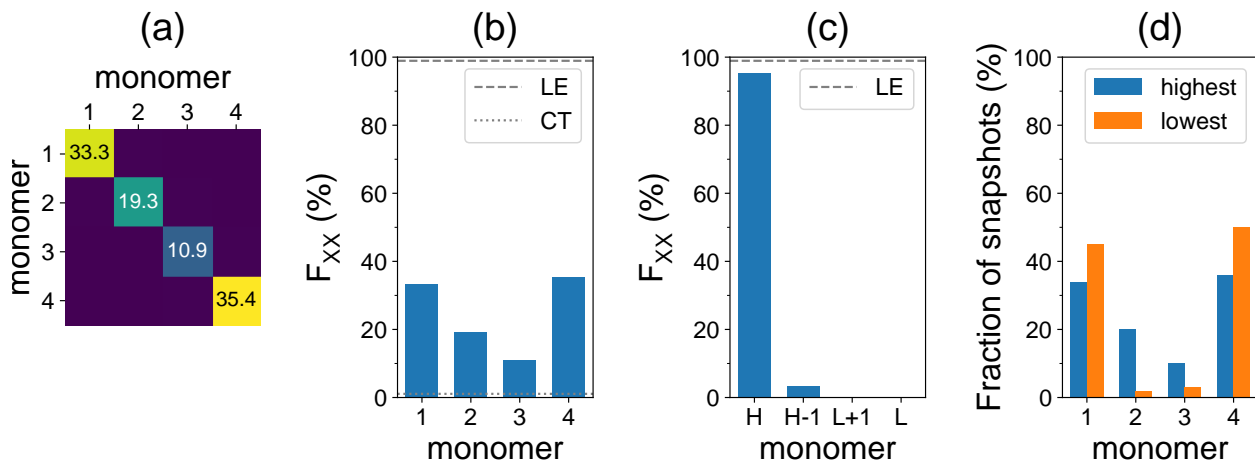


Figure S35: TD- ω B97X-D/def2-SV(P) calculations, $T \approx 300$ K. (a) The \mathbf{F} matrix averaged over all snapshots. (b) Diagonal F_{XX} elements of the averaged \mathbf{F} matrix, as well as the sum of diagonal (LE) and off-diagonal (CT) elements. (c) Averaged highest to lowest diagonal values and their sum (LE). (d) Relative frequency with which monomers have the highest or lowest F_{XX} value.

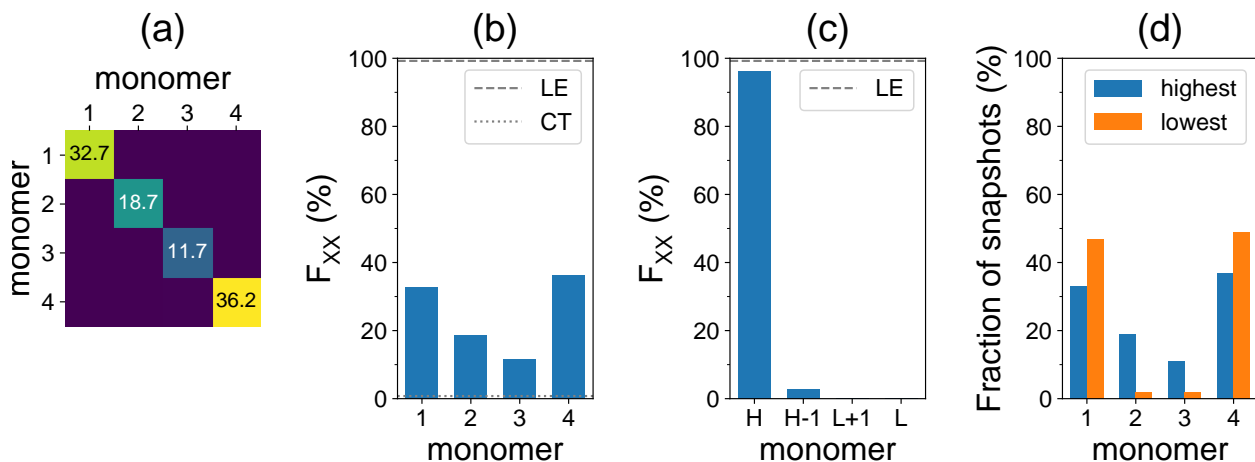


Figure S36: TD- ω B97/def2-SV(P) calculations, $T \approx 300$ K. (a) The \mathbf{F} matrix averaged over all snapshots. (b) Diagonal F_{XX} elements of the averaged \mathbf{F} matrix, as well as the sum of diagonal (LE) and off-diagonal (CT) elements. (c) Averaged highest to lowest diagonal values and their sum (LE). (d) Relative frequency with which monomers have the highest or lowest F_{XX} value.

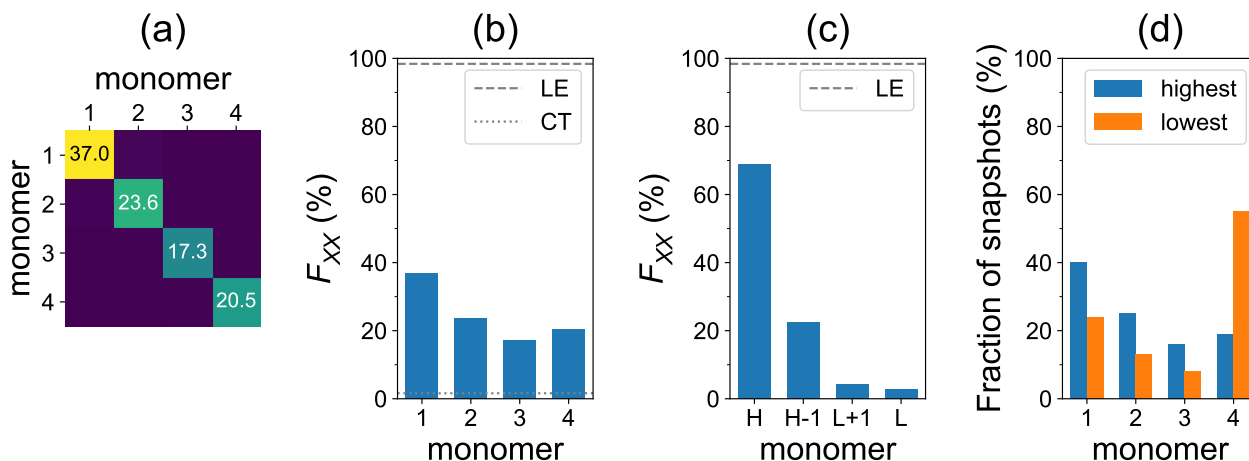


Figure S37: TD- ω B97X-D/def2-SV(P) calculations, $T < 26$ K. (a) The \mathbf{F} matrix averaged over all snapshots. (b) Diagonal F_{XX} elements of the averaged \mathbf{F} matrix, as well as the sum of diagonal (LE) and off-diagonal (CT) elements. (c) Averaged highest to lowest diagonal values and their sum (LE). (d) Relative frequency with which monomers have the highest or lowest F_{XX} value.

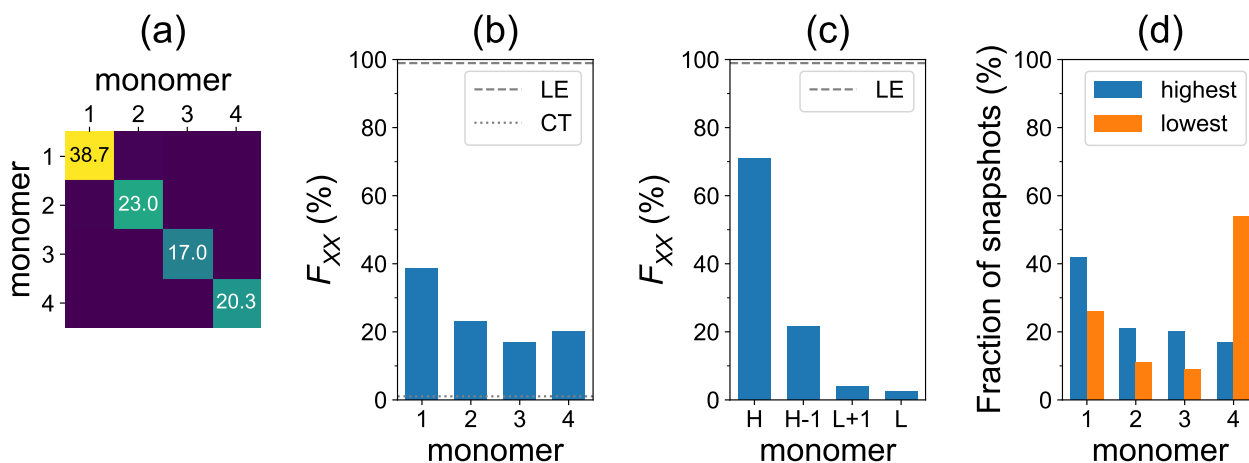


Figure S38: TD- ω B97/def2-SV(P) calculations, $T < 26$ K. (a) The \mathbf{F} matrix averaged over all snapshots. (b) Diagonal F_{XX} elements of the averaged \mathbf{F} matrix, as well as the sum of diagonal (LE) and off-diagonal (CT) elements. (c) Averaged highest to lowest diagonal values and their sum (LE). (d) Relative frequency with which monomers have the highest or lowest F_{XX} value.

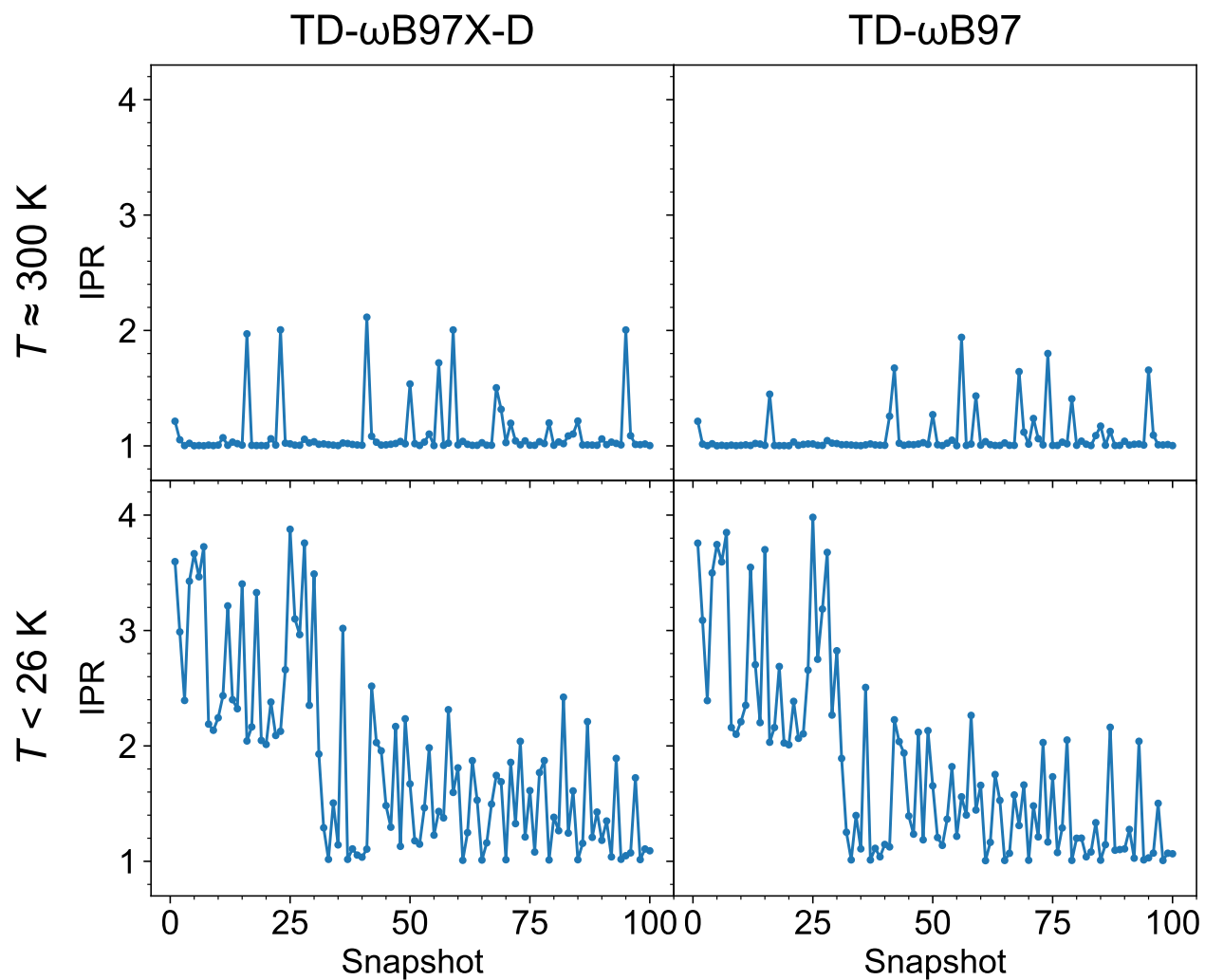


Figure S39: Inverse participation ratios for 100 snapshots.

